Relationship between Viscosity and Acyl Tail Dynamics in Lipid Bilayers

Michihiro Nagao, Elizabeth G. Kelley, Antonio Faraone, Makina Saito, Yoshitaka Yoda, Masayuki Kurokuzu, Shinichi Takata, Makoto Seto, and Paul D. Butler

Relationship between viscosity and acyl tail dynamics in lipid bilayers

Michihiro Nagao,[1, 2, 3, *] Elizabeth G. Kelley,[1] Antonio Faraone,[1] Makina Saito,[4, †] Yoshitaka Yoda,[5] Masayuki Kurokuzu,[4] Shinichi Takata,[6] Makoto Seto,[4] and Paul D. Butler[1, 7, 8]

[1] National Institute of Standards and Technology Center for Neutron Research, Gaithersburg, Maryland, USA.
[2] Department of Materials Science and Engineering,
University of Maryland, College Park, Maryland, USA.
[3] Department of Physics and Astronomy, University of Delaware, Newark, Delaware, USA.
[4] Institute for Integrated Radiation and Nuclear Science, Kyoto University, Kumatori, Osaka, Japan
[5] Japan Synchrotron Radiation Research Institute, Sayo, Hyogo, Japan
[6] J-PARC Center, Japan Atomic Energy Agency, Tokai, Ibaraki, Japan
[7] Department of Chemical and Biomolecular Engineering,
University of Delaware, Newark, Delaware, USA
[8] Department of Chemistry, The University of Tennessee, Knoxville, Tennessee, USA
(Dated: June 29, 2021)

Membrane viscosity is a fundamental property that controls molecular transport and structural rearrangements in lipid membranes. Given its importance in many cell processes, various experimental and computational methods have been developed to measure the membrane viscosity, yet the estimated values depend highly on the method and vary by orders of magnitude. Here we investigate the molecular origins of membrane viscosity by measuring the nanoscale dynamics of the lipid acyl tails using X-ray and neutron spectroscopy techniques. The results show that the membrane viscosity can be estimated from the structural relaxation times of the lipid tails.

Biomembranes are unique platforms for various biological processes and functions via the structural and dynamical coupling between proteins and lipid molecules. [1] The lipid bilayer that forms these membranes serves as a fluid matrix that facilitates interactions between individual lipids and proteins, formation of domains, and reorganization of membrane components to form multimeric signalling complexes. Understanding the transport properties of two-dimensional lipid membranes, therefore, is both fundamentally interesting and biologically relevant.

Viscosity is an intrinsic material property that characterizes the transport of momentum in a material. While methods for determining the viscosity in three-dimensional fluids are well established; measuring the viscosity of two dimensional membranes is much more challenging, yet equally important. Experimentally, techniques such as falling ball viscometry and optical dynanometry have been used to estimate the membrane hydrodynamic shear viscosity by estimating the friction felt by a particle on a vesicle surface or tracking the movement of a particle stuck to the surface of a lipid vesicle, where the viscosity is defined on a scale significantly larger than the structural details of the membrane. [2–5] Similarly, studies of dynamic critical phenomena [6] or measurements that track tracer, domain, or particle diffusion that estimate the membrane viscosity from the measured probe diffusion [7–13] also use hydrodynamic models. [14–18] Such treatments, however, break down as the inclusion size decreases and the continuum picture of the membrane becomes untenable. [19, 20] Other techniques determine membrane viscosity via non-equilibrium methods such as using pipettes to pull tethers [21] and measuring the micro- and surface-rheology of giant vesicles. [22, 23] Computer simulations using non-equilibrium shear stress methods also have been developed to predict membrane viscosity. [24–26] Recently, our group has established a methodology to calculate the membrane viscosity from the equilibrium collective thermal fluctuations of membranes by means of quasi-elastic neutron scattering (QENS). [27–31] However, estimates for the membrane viscosity vary by orders of magnitude depending on the experimental method used, highlighting the need for a more detailed understanding of the molecular origins of membrane viscosity.

Even in three dimensional liquid systems, understanding the molecular origins of viscosity is fundamentally complex due to the different length and time scales of the interactions between molecules. Experimentally, coherent QENS experiments have shown that structural relaxation time, τ, measured at a structural correlation peak of molecular liquids follows the same temperature T dependence as the liquid viscosity η, namely $\tau \propto \eta/T$. [32–35] This relation suggests a universal feature in that the friction within liquids likely originates from the structural rearrangements of the constituent molecules. The Green-Kubo theory [36, 37] describes the molecular origins of viscosity as a time-correlation function of the stress tensor, and recent studies using this theory suggest that the structural relaxations (dynamics of the density correlations) in simple liquids are the main determinant of the viscosity. [38] In two dimensional membrane systems, however, there are no known attempts to either experimentally or theoretically verify the molecular mechanism underlying membrane viscosity.

* mnagao@umd.edu
† Current address: Department of Physics, Graduate School of Science, Tohoku University, Sendai, Miyagi, Japan

In this study, we employ neutron and X-ray scattering techniques to measure the collective dynamics of lipid acyl tails at the structural correlation peak and demonstrate that these molecular dynamics can be linked to the membrane viscosity as reported for simple liquid systems. Lipid molecules are known to show a structural correlation peak around a scattering vector $q = 4\pi \sin(\theta/2)/\lambda \approx 1.5$ Å^{-1} with θ and λ being scattering angle and incoming probe wavelength, respectively, which corresponds to a correlation distance of approximately 4.5 Å. [39] The peak originates from the acyl tail correlations and is often used to describe structural order of the individual lipid molecules within the membrane. [40] The peak sharpness depends on the lipid molecular structural order and is indicative of the lipid phase. In the gel (L$_{\beta'}$) or rippled gel (P$_{\beta'}$) phases, the acyl tails are highly-ordered, giving a distinct and sharp scattering peak. [41] In contrast, in the fluid (L$_\alpha$) phase, the lipid acyl tails are more disordered and the corresponding correlation peak is broader. Figure S1a of the Supplemental Material [42] shows a typical example of neutron diffraction data from the P$_{\beta'}$ and L$_\alpha$ phases measured on TAIKAN at J-PARC, [43] for tail-deuterated dimyristoyl phosphatidylcholine (DMPC-d$_{54}$) in D$_2$O. In the present study, the collective motions of the lipid hydrocarbons near this structural correlation peak were measured with a combination of neutron spin echo (NSE) spectroscopy and Mössbauer time-domain interferometry (MTDI) over more than 4 orders of magnitude in time ranging from a few ps to 300 ns.

The temperature dependence of the acyl tail dynamics in DMPC lipid membranes were measured in water in the three distinct L$_{\beta'}$, P$_{\beta'}$, and L$_\alpha$ lipid phases. Samples were multilamellar vesicles prepared from either protiated DMPC in H$_2$O or DMPC-d$_{54}$ in D$_2$O for the X-ray and neutron scattering experiments, respectively. The lipid concentration was fixed at 400 mg/mL. [44] The NSE experiment was performed using the NGA-NSE spectrometer at the NIST Center for Neutron Research, [45, 46] and the MTDI experiment was performed on BL09XU at SPring-8. [47] Both NSE and MTDI yield the normalized intermediate scattering function, $I(q,t)/I(q,0)$, which is the spatial Fourier transform of the van-Hove space time correlation function. Details of the experiments are presented in the Supplemental Material. [42]

Figure 1a and b show the temperature dependence of the $I(q,t)/I(q,0)$ measured by NSE and by MTDI, respectively, at $q \approx 1.5$ Å^{-1}, that we attribute to the structural relaxations of the lipid acyl tails. The NSE data at timescales ≤ 16 ns were corrected for contributions from the D$_2$O solvent in this time window and thus reflect the relaxation behavior of the lipid acyl tails. On the other hand, the MTDI data were measured at much longer time scales than the NSE, and the water dynamics have completely relaxed at these longer times. [35] As such, the measured relaxation behaviors in the MTDI spectra also correspond to the lipid acyl tail dynamics. The contribution from water dynamics is only seen in the
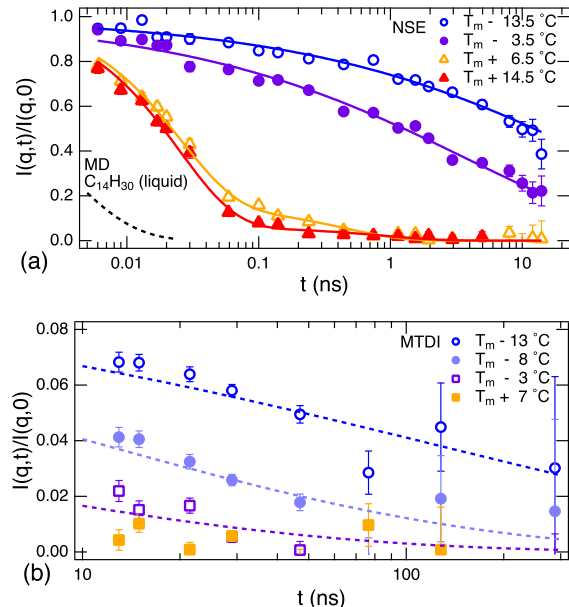

FIG. 1. (Color online) (a) Normalized intermediate scattering function $I(q,t)/I(q,0)$ measured with NSE for DMPC-d$_{54}$/D$_2$O. Relative temperature to $T_{m_{d54}} = 20.5$ °C [48] is shown in the legend. The solid lines are the fit results according to a KWW function for the data at $T \leq T_{m_{d54}}$ and a double exponential function above $T_{m_{d54}}$. The dashed line is the relaxation behavior at the structure factor peak for bulk tetradecane, C$_{14}$H$_{30}$, determined from molecular dynamics simulations. [38] (b) $I(q,t)/I(q,0)$ for DMPC/H$_2$O measured with MTDI. Relative temperature to $T_{m_H} = 24$ °C is shown in the legend. The lines are the fit results according to a KWW function with the stretching exponent fixed to $\beta = 0.33$ as estimated from the NSE results. Error bars represent ± 1 standard deviation throughout the paper.

amplitude of the lipid relaxation mode in the MTDI data (the initial value of $I(q,t)/I(q,0)$ at short times). The NSE and MTDI data for the lipid dynamics are plotted separately in Figure 1 because of the differences in how the water background were treated. The scaled MTDI data are also presented in Figure S3c [42] as a combined plot with the NSE data to better visualize the relaxation behavior over the entire studied time window.

The NSE data (Fig. 1a) indicated the presence of a single slow relaxation in the gel phase (below the main transition temperature $T_{m_{d54}} = 20.5$ °C [48]). The data were fit with a Kohlrausch-Williams-Watts (KWW) function (equation S3 [42]), and the corresponding average relaxation times $\langle \tau_{NSE} \rangle$ were estimated (equation S4 [42]). Meanwhile, in the L$_\alpha$ phase at $T \geq T_{m_{d54}}$, two relaxation processes were identified, and a double exponential function (equation S5 [42]) was used to fit the data and determine the relaxation times for the fast, τ_f, and slow, τ_s, modes. More detailed explanations of the fitting procedures can be found in section S2. [42] The extracted fit parameters are summarized in Figure 2 and Table S2 and S3. [42]
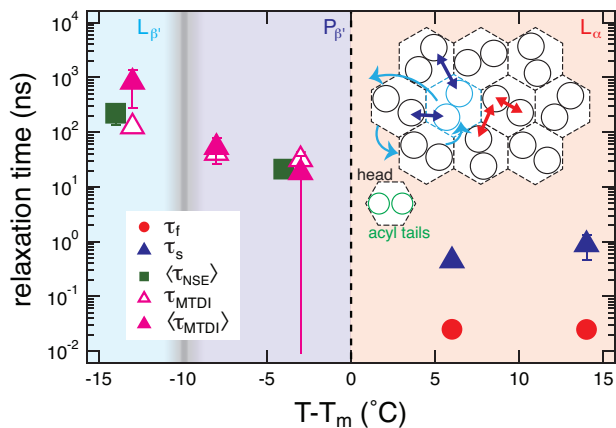
FIG. 2. (Color online) Estimated relaxation times $\langle\tau_{NSE}\rangle$, τ_{MTDI} and $\langle\tau_{MTDI}\rangle$ in the gel phase and the fast τ_f and slow τ_s relaxation times in the fluid phase. The vertical lines indicate the boundaries between the $L_{\beta'}$ to $P_{\beta'}$ phases at the pre-transition temperature ($T_p \approx 11\ °C$), and between the $P_{\beta'}$ to L_α phases. The horizontal axis displays the relative temperature from the lipid main phase transition temperature, T_m, which is about 4 °C different between protiated DMPC and DMPC-d_{54}. The schematic in the inset illustrates the proposed trajectories of the two-dimensionally distributed lipid molecules. The dashed hexagonal area indicates the area occupied by a lipid head group, while circles represent projections of lipid acyl tails. The faster relaxation likely originates from the rearrangements of the acyl tails (represented by the red double arrows), while the slower mode is associated with the motion of an entire lipid molecule (light blue arrows). The dark blue double arrows represent the acyl tail correlations that are affected by the lipid molecular motions and their rearrangements, and are considered as the origin of the slow mode.

The relaxation times determined from the current experiments were compared with results from a previous neutron backscattering (BS) measurement also for DMPC lipid membranes, but for membranes prepared in a different geometry (supported bilayers). [49] In the L_α phase, Rheinstädter and colleagues identified two relaxation processes, faster dynamics with $\tau_f^{BS} \approx 0.1$ ns or less and a slower process with $\tau_s^{BS} \approx 0.5$ ns. These values agree reasonably well with the results from the present experiment for the L_α phase, with $\tau_f \approx 0.03$ ns and $\tau_s \approx 0.5$ ns. In the gel phase, on the other hand, the previous BS results suggested that $\tau_f^{BS} \approx 0.1$ ns and $\tau_s^{BS} \approx 1$ ns, which are much faster than the relaxation times determined from our NSE and MTDI measurements. This discrepancy is likely because the slow and heterogeneous dynamics in the gel phase (the stretching exponent from the current NSE results was $\beta \approx 0.3$) exceeded the energy resolution and dynamic window of the previous BS experiment. Thus, the observed dynamics in the previous BS experiment may have been dominated by contributions from the water dynamics.

The measured time spectra from the MTDI experiments were analyzed as shown in section S3 [42], and

the corresponding $I(q,t)/I(q,0)$ estimated from the time spectra are plotted in Figure 1b. The MTDI data for the gel phase membranes were reasonably well fit using the stretching exponent $\beta = 0.33$ determined from fits to the NSE data, and the average relaxation times $\langle\tau_{MTDI}\rangle$ were determined. [50] As shown in Figure 2, the estimated relaxation times were comparable for both the NSE and MTDI analyses. These results suggest that the dynamics observed by NSE and MTDI in the gel phase were due to the same relaxation process, and only one relaxation mode was identified at $T < T_m$ in the present study. The dynamics at $T = 31$ °C were fully relaxed in the MTDI time window as also supported by the NSE data. The relaxation time in the gel phase was more than an order of magnitude slower than the slow mode in the L_α phase (τ_s) as seen in Figure 2, which is consistent with the knowledge that the dynamics are more than an order of magnitude slower in the gel phase than the fluid phase. [48]

Here, we consider the molecular origins of the relaxation modes measured at the acyl tail correlation peak. The relaxation times of the two modes identified in the L_α phase vary by an order of magnitude and likely have different molecular origins. We attribute the fast mode with $\tau \approx 0.03$ ns to the structural rearrangements of the individual lipid acyl tails while the slower mode with $\tau \approx 0.5$ ns likely corresponds to the entire lipid molecule escaping from its molecular cage as discussed below. The fit values for the relative amplitudes of the two modes indicated that the fast mode was more prevalent.

It is interesting to compare the structural relaxation dynamics of the lipid acyl tails in the bilayers to the corresponding bulk liquid n-alkane to see how the two-dimensional confinement of the hydrocarbon chains affects their motions. Because the present experiments used DMPC (diC14 PC) lipids, we compare the results for the lipid membranes with the analogous linear alkane, tetradecane ($C_{14}H_{30}$), as a simple model for the hydrocarbon chain. While, to the best of our knowledge there are not reported QENS measurements of the relaxation dynamics at the $C_{14}H_{30}$ structure factor peak, recent computer simulations of these dynamics successfully determined the experimentally observed macroscopic shear viscosity from the microscopic structural relaxations.[38] The corresponding relaxation time for bulk $C_{14}H_{30}$ was $\tau_{MD} \approx 0.003$ ns, [38] which is about an order of magnitude faster than even the fastest mode measured for the DMPC acyl tails, ($\tau_f \approx 0.03$ ns). This comparison suggests that the two-dimensional confinement and orientational ordering of the $C_{14}H_{30}$ hydrocarbon chains as well as the restricted motions due to the binding of one end of the chain to the headgroup significantly slows the chain relaxations.

As suggested above, the slower mode likely originates from the entire lipid escaping from its cage and rearranging with neighboring lipid molecules. In this case, the slow mode should be related to the diffusive motion of the lipid molecules outside the molecular cage, similar to

the long length scale lipid molecular diffusion measured with fluorescent probe techniques [19] or nuclear magnetic resonance (NMR) spectroscopy. [51] NMR measurements of DMPC lipid diffusion gave $D \approx 1 \times 10^{-11}$ m^2/s at $T = 308$ K, [51] which corresponds to a relaxation time, $\tau = 1/(Dq^2) \approx 0.45$ ns. Quite interestingly, this estimate is in good agreement with $\tau_s \approx 0.5$ ns from the structural relaxations measured here.

Meanwhile, below T_m, both the fast and slow modes are expected to significantly slow down. As a result, the structural relaxation dynamics likely become much more heterogeneous, which would then lead to the observed stretched exponential decay with a relatively small value of the stretching exponent, $\beta \approx 0.3$.

While theories relating the structural relaxations of the lipid acyl tails to the viscosity of two-dimensional fluid membranes have not yet been developed, we can borrow ideas developed from studies of three-dimensional simple liquids, where $\tau \propto \eta/T$. This scaling relationship indicates that when the density correlations in the system relax slowly (large τ), the momentum transport is also slow (large η). We assume that this scaling is true in the liquid state of the hydrocarbon chains in a lipid membrane as well. The viscosity of DMPC in three dimension then would be expressed as $\eta_L = (\tau_L/\tau_{MD})(T_L/T_0)\eta_0$ by comparing the dynamics in C$_{14}$H$_{30}$ and DMPC, where τ_L and T_L are the relaxation time and temperature in the present experiments, the viscosity of C$_{14}$H$_{30}$ is $\eta_0 = 2.73$ mPa·s at $T_0 = 25$ °C, [52] and $\tau_{MD} \approx 3$ ps. [38]

The surface viscosity η_m of a thin sheet of a homogeneous liquid is expressed as $\eta_m = d\eta$ where d and η are the thickness of the thin sheet and bulk liquid viscosity, respectively. [16] Applying $d_c = 3.5$ nm for a DMPC bilayer, [31] η_m is calculated as $\eta_m = d\eta_L$, and the corresponding values are plotted in Figure 3 together with various membrane viscosity values estimated experimentally and computationally in literature. [4, 11, 24, 25, 28, 38, 53, 54] The estimate of η_m from τ_f is on the order of 0.1 nPa·s·m. This value is an order of magnitude lower than the membrane viscosity measured with fluorescent probe techniques, [11, 53] suggesting that the structural rearrangements of the lipid acyl tails are not related to the membrane viscosity measured in such experiments. On the other hand, $\eta_m \sim 1$ nPa·s·m calculated from the slower relaxation time τ_s is in good agreement with membrane viscosity values determined using probe diffusion methods and close to the median of the wide range of η_m values reported in literature. Therefore, the present results provide experimental evidence that the structural relaxation dynamics associated with the lipids escaping from their molecular cage and rearranging with the surrounding lipid molecules are related to the membrane viscosity.

The combination of the NSE and MTDI results suggests η_m varies significantly with temperature in the gel phase. As discussed by den Otter and Shkulipa, [25] the lipid molecular order has a considerable impact on the membrane viscosity, and the present results directly
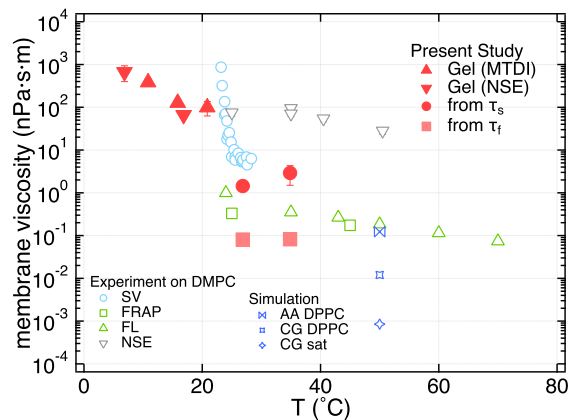

FIG. 3. (Color online) Comparison of membrane viscosity values reported in literature (open points) and estimated values from the present results for the relaxation times of the acyl chains (solid points). Experimental data for DMPC are from the surface viscometry (SV) [4], fluorescence recovery after photobleaching (FRAP), [53] fluorescent lifetime measurements (FL), [11] and NSE measurements (NSE). [28, 55] Computer simulations have been used to calculate saturated lipid with coarse-grained simulation (CG sat) [24], dipalmitoylphosphatidylcholine (DPPC) model with CG (CG DPPC) [25], and all atom simulation of DPPC (AA DPPC). [54] A more thorough comparison of the present results to other values of η_m reported for various lipids in literature is shown in Figure S4. [42]

show that the acyl tail dynamics depend significantly on the lipid phase. Similarly, surface viscometry measurements by Dimova et $al.$ showed a significant increase in the membrane viscosity in the fluid phase of DMPC giant unilamellar vesicles near T_m that they attributed to pretransitional structural fluctuations in the membrane, $i.e.$, an inhomogeneous structure composed of a mixture of fluid- and gel-like domains. [4] Such long range gel-like domains may easily prevent macroscopic particle motions even in the fluid phase, while the present results show that nanoscale molecular motions still survive even as the temperature is lowered into the gel phase and the membranes are increasingly solidified at the molecular level as temperature is decreased.

In simple liquid systems, the Green-Kubo formula predicts a relationship between the frequency dependent shear viscosity, which has been related to the intermediate scattering function and the molecular structural relaxations by employing concepts from mode coupling theory. [38, 56–58] The present results suggest that these concepts from three-dimensional liquid systems may also apply to two-dimensional fluid membrane systems, and theoretical developments in two dimension are highly desirable to clarify and refine the present methodology for calculating membrane viscosity from the acyl tail structural relaxations as suggested here.

Together, the combination of NSE and MTDI accessed structural relaxation of lipid acyl tails over more than 4

orders of magnitude in time. This is a unique opportunity offered by the combination of the neutron and X-ray spectroscopic techniques and provide new insights into the collective acyl tail dynamics. The NSE data provided access to the nanosecond relaxation times expected for the acyl tails, while the MTDI data extend the probed time window to a range relevant for the gel phases. The data showed that the two dimensional confinement of the lipid acyl tails slowed their dynamics by more than an order of magnitude compared to three dimensional liquids. The results further revealed that the acyl tail dynamics directly link the macroscopic transport properties in lipid membranes that can affect cell function and perhaps one day offer new 'membrane lipid therapies' that seek to control the physical properties of lipid membranes. [59–61] We hope that the present results inspire further experimental, computational, and theoretical studies into the molecular origins of membrane viscosity.

[1] E. Sezgin, I. Levental, S. Mayor, and C. Eggeling, The mystery of membrane organization: composition, regulation and roles of lipid raft, Nat. Rev. Mol. Cell Biol. **18**, 361 (2017).

[2] K. Danov, R. Aust, F. Durst, and U. Lange, Influence of the surface viscosity on the hydrodynamic resistance and the surface diffusivity of a large brownian particle, J. Colloid Interface Sci. **175**, 36 (1995).

[3] R. Dimova, C. Dietrich, A. Hadjisky, K. Danov, and B. Pouligny, Falling ball viscosimetry of giant vesicle membranes: Finite-size effects, Eur. Phys. J. B **12**, 589 (1999).

[4] R. Dimova, B. Pouligny, and C. Dietrich, Pretransitional effects in dimyristoylphosphatidylcholine vesicle membranes: Optical dynamometry study, Biophys. J. **79**, 340 (2000).

[5] K. D. Danov, R. Dimova, and B. Pouligny, Viscous drag of a solid sphere straddling a spherical or flat surface, Phys. Fluids **12**, 2711 (2000).

[6] A. R. Honerkamp-Smith, B. B. Machta, and S. L. Keller, Experimental observations of dynamic critical phenomena in a lipid membrane, Phys. Rev. Lett. **108**, 265702 (2012).

[7] P. Cicuta, S. L. Keller, and S. L. Veatch, Diffusion of liquid domains in lipid bilayer membranes, J. Phys. Chem. B **111**, 3328 (2007).

[8] M. E. Nipper, S. Majd, M. Mayer, J. C. M. Lee, E. A. Theodorakis, and M. A. Haidekker, Biochim. Biophys. Acta **1778**, 1148 (2008).

[9] B. A. Camley, C. Esposito, T. Baumgart, and F. L. H. Brown, Lipid bilayer domain fluctuations as a probe of membrane viscosity, Biophys. J. **99**, L44 (2010).

[10] A. R. Honerkamp-Smith, F. G. Woodhouse, V. Kantsler, and R. E. Goldstein, Membrane viscosity determined from shear-driven flow in giant vesicles, Phys. Rev. Lett. **111**, 038103 (2013).

[11] Y. Wu, M. Stefl, A. Olzynska, M. Hof, G. Yahioglu, P. Yip, D. R. Casey, O. Ces, J. Humpolickova, and M. K. Kulmova, Molecular rheometry: direct determination of viscosity in L_o and L_d lipid phase *via* fluorescence lifetime imaging, Phys. Chem. Chem. Phys. **15**, 14986 (2013).

[12] T. T. Hormel, S. Q. Kurihara, M. K. Brennan, M. C. Wozniak, and R. Parthasarathy, Measuring lipid membrane viswcosity using rotational and translational probe diffusion, Phys. Rev. Lett. **112**, 188101 (2014).

[13] Y. Sakuma, T. Kawakatsu, T. Taniguchi, and M. Imai, Viscosity landscape of phase-separated lipid membranes estimated from fluid velocity field, Biophys. J. **118**, 1576 (2020).

[14] P. G. Saffman and M. Delbrück, Brownian motion in biological membranes, Proc. Natl. Acad. Sci. USA. **72**, 3111 (1975).

[15] B. D. Hughes, B. A. Pailthorpe, and L. R. White, The translational and rotational drag on a cylinder moving in a membrane, J. Fluid Mech. **10**, 349 (1981).

[16] E. Evans and E. Sackmann, Translational and rotational drag coefficients for a disk moving in a liquid membrane associated with a rigid substrate, J. Fluid Mech. **194**, 553 (1988).

[17] M. L. Henle and A. J. Levine, Hydrodynamics in curved membranes: the effect of geometry on particulate mobility, Phys. Rev. E **81**, 011905 (2010).

[18] B. A. Camley and F. L. H. Brown, Diffusion of complex objects embedded in free and supported lipid bilayer membranes: role of shape anisotropy and leaflet structure, Soft Matter **9**, 4767 (2013).

[19] W. L. C. Vaz, T. B. Clegg, and D. Hallmann, Translational diffusion of lipids in liquid crystalline phase phosphatidylcholine multibilayers. A comparison of experiment with theory, Biochem. **24**, 781 (1985).

[20] B. A. Camley and F. L. H. Brown, Contributions to membrane-embedded-protein diffusion beyond hydrodynamic theories, Phys. Rev. E **85**, 061921 (2012).

[21] R. E. Waugh, Biophys. J. **38**, 29 (1982).

[22] C. W. Harland, M. J. Bradley, and R. Parthasarathy, Phospholipic bilayers are viscoelastic, Proc. Natl. Acad. Sci. USA. **107**, 19146 (2010).

[23] G. Espinosa, I. Lopez-Montero, F. Monroy, and D. Langevin, Proc. Natl. Acad. Sci. USA. **108**, 6008 (2011).

[24] S. A. Shkulipa, W. K. den Otter, and W. J. Briels, Surface viscosity, diffusion, and intermonolayer friction: sim-

ulating sheared amphiphilic bilayers, Biophys. J. **89**, 823 (2005).

[25] W. K. den Otter and S. A. Shkulipa, Intermonolayer friction and surface shear viscosity of lipid bilayer membranes, Biophys. J. **93**, 423 (2007).

[26] A. Zgorski and E. Lyman, Toward hydrodynamics with solvent free lipid models: STRD martini, Biophys. J. **111**, 2689 (2016).

[27] R. Bradbury and M. Nagao, Effect of charge on the mechanical properties of surfactant bilayers, Soft Matter **12**, 9383 (2016).

[28] M. Nagao, E. G. Kelley, R. Ashkar, R. Bradbury, and P. D. Butler, Probing elastic and viscous properties of phospholipid bilayers using neutron spin echo spectroscopy, J. Phys. Chem. Lett. **8**, 4679 (2017).

[29] E. G. Kelley, P. D. Butler, and M. Nagao, Collective dynamics in model biological membranes measured by neutron spin echo spectroscopy, in *Characterization of Biological Membranes - Structure and Dynamics*, edited by J. Katsaras, M. P. Nieh, and F. A. Heberle (de Gruyter, 2019) Chap. 4, pp. 131–176.

[30] S. Chakraborty, M. Doktorova, T. R. Molugu, F. A. Heberle, H. L. Scott, B. Dzikovski, M. Nagao, L. R. Stingaciu, R. F. Standaert, F. N. Barrera, J. Katsaras, G. Khelashvili, M. F. Brown, and R. Ashkar, How cholesterol stiffens unsaturated lipid membranes, Proc. Natl. Acad. Sci. USA. **117**, 21896 (2020).

[31] E. G. Kelley, P. D. Butler, R. Ashkar, R. Bradbury, and M. Nagao, Scaling relationships for the elastic moduli and viscosity of mixed lipid membranes, Proc. Natl. Acad. Sci. USA. **117**, 23365 (2020).

[32] F. Mezei, W. Knaak, and B. Farago, Neutron spin echo study of dynamic correlations near the liquid-glass transition, Phys. Rev. Lett. **58**, 571 (1987).

[33] J. Wuttke, W. Petry, and S. Pouget, Structural relaxation in viscous glycerol: Coherent neutron scattering, J. Chem. Phys. **105**, 5177 (1996).

[34] T. Yamaguchi, K. Yoshida, T. Yamaguchi, M. Nagao, A. Faraone, and S. Seki, Decoupling between the temperarture-dependent structural relaxation and shear viscosity of concentrated lithium electrolyte, J. Phys. Chem. B **121**, 8767 (2017).

[35] A. Yahya, L. Tan, S. Perticaroli, E. Mamontov, D. Pajerowski, J. Neuefeind, G. Ehlers, and J. D. Nickels, Molecular origins of bulk viscosity in liquid water, Phys. Chem. Chem. Phys. **22**, 9494 (2020).

[36] M. S. Green, Markoff random processes and the statistical mechanics of time-dependent phenomena. II. Irreversible processes in fluids, J. Chem. Phys. **22**, 398 (1954).

[37] R. Kubo, Statistical-mechanical theory of irreversible processes. I. General theory and simple applications to magnetic and conduction problems, J. Phys. Soc. Jpn. **12**, 570 (1957).

[38] T. Yamaguchi, Viscoelastic relaxations of high alcohols and alkanes: Effects of heterogeneous structure and translation-orientation coupling, J. Chem. Phys. **146**, 094511 (2017).

[39] J. S. Hub, T. Salditt, M. C. Rheinstädter, and B. L. de Groot, Short-range order and collective dynamics of DMPC bilayers: A comparison between molecular dynamics simulations, X-ray, and neutron scattering experiments, Biophys. J. **93**, 3156 (2007).

[40] T. T. Mills, G. E. S. Toombes, S. Tristram-Nagle, D. M. Smilgies, G. W. Feigenson, and J. F. Nagle, Order parameters and areas in fluid-phase oriented lipid membranes using wide angle X-ray scattering, Biophys. J. **95**, 669 (2008).

[41] K. Akabori and J. F. Nagle, Structure of the DMPC lipid bilayer ripple phase, Soft Matter **11**, 918 (2015).

[42] See Supplemental Material [url] for details on the experimental methods and data treatment as well as a more comprehensive comparison with membrane viscosity values reported in literature, which includes refs. [62–70].

[43] S. Takata, J. Suzuki, T. Shinohara, T. Oku, T. Tominaga, K. Ohishi, H. Iwase, T. Nakatani, Y. Inamura, T. Ito, K. Suzuya, K. Aizawa, M. Arai, T. Otomo, and M. Sugiyama, The design and q resolution of the small and wide angle neutron scattering instrument (TAIKAN) in J-PARC, J. Phys. Soc. Conf. Proc. **8**, 036020 (2015).

[44] A more appropriate choice for the sample composition may have been to keep the same number concentration of lipid molecules. However, we do not expect this small difference (about 7 %) to affect the final results.

[45] M. Monkenbusch, R. Schatzler, and D. Richter, The jülich neutron spin-echo spectrometer - design and performance, Nucl. Instrum. Meth. Phys. Res., A **399**, 301 (1997).

[46] N. Rosov, S. Rathgeber, and M. Monkenbusch, Neutron spin echo spectroscopy at the NIST center for neutron research, ACS Symp. Ser. **739**, 103 (1999).

[47] M. Saito, R. Masuda, Y. Yoda, and M. Seto, Synchrotron radiation-based quasi-elastic scattering using time-domain interferometry with multi-line gamma rays, Sci. Rep. **7**, 12558 (2017).

[48] A. C. Woodka, P. D. Butler, L. Porcar, B. Farago, and M. Nagao, Lipid bilayers and membrane dynamics: Insight into thickness fluctuations, Phys. Rev. Lett. **109**, 058102 (2012).

[49] M. C. Rheinstädter, J. Das, E. J. Flenner, B. Brüning, T. Seydel, and I. Kosztin, Motional coherence in fluid phospholipid membranes, Phys. Rev. Lett. **101**, 248106 (2008).

[50] Independent analyses assuming that the MTDI data followed single exponential relaxation dynamics ($\beta = 1$) were also performed to get the relaxation time τ_{MTDI} as shown in Figure S2b. [42].

[51] A. Filippov, G. Orädd, and G. Lindblom, The effect of cholesterol on the lateral diffusion of phospholipids in oriented bilayers, Biophys. J. **84**, 3079 (2003).

[52] W. M. Haynes, ed., *CRC Handbook of Chemistry and Physics* (CRC Press LLC, 2014-2015).

[53] R. Merkel, E. Sackmann, and E. Evans, Molecular friction and epitactic coupling between monolayers in supported bilayers, J. Phys. France **50**, 1535 (1989).

[54] A. Zgorski, R. W. Pastor, and E. Lyman, Surface shear viscosity and interleaflet friction from nonequilibrium simulations of lipid bilayers, J. Chem. Theory Comput. **15**, 6471 (2019).

[55] The values of η_m in [28] were estimated from the thickness fluctuation relaxation dynamics. These fluctuations may be affected by internal dissipation within the membrane that has not yet been incorporated into the data analysis framework. This point will be discussed in more detail in our future publications, but we expect that η_m values in [28] may have been overestimated.

[56] T. Yamaguchi and F. Hirata, Site–site mode-coupling theory for the shear viscosity of molecular liquids, J.

Chem. Phys. **115**, 9340 (2001).

[57] T. Yamaguchi and S. Koda, Mode-coupling theoretical analysis of transport and relaxation properties of liquid dimethylimidazolium chloride, J. Chem. Phys. **132**, 114502 (2010).

[58] T. Yamaguchi, K. Mikawa, S. Koda, K. Fujii, H. Endo, M. Shibayama, H. Hamano, and Y. Umebayashi, Relationship between mesoscale dynamics and shear relaxation of ionic liquids with long alkyl chain, J. Chem. Phys. **137**, 104511 (2012).

[59] P. V. Escribá, Membrane-lipid therapy: a new approach in molecular medicine, Trend. Mol. Med. **12**, 34 (2006).

[60] P. V. Escribá, Membrane-lipid therapy: A historical perspective of membrane-targeted therapies - from lipid bilayer structure to the pathophysiological regulation of cells, Biochim. Biophys. Acta **1859**, 1493 (2017).

[61] L. T. H. Tan, K. G. Chan, P. Pusparajah, W. L. Lee, L. H. Chuah, T. M. Khan, L. H. Lee, and B. H. Goh, Targeting membrane lipid a potential cancer cure?, Front. Pharmacol. **8**, 12 (2017).

[62] F. Mezei, Neutron spin echo: A new concept in polarized thermal neutron techniques, Z. Physik **255**, 146 (1972).

[63] R. Azuah, L. Kneller, Y. Qiu, P. Tregenna-Piggott, C. Brown, J. Copley, and R. Dimeo, DAVE: A comprehensive software suite for the reduction, visualization, and analysis of low energy neutron spectroscopic data, J. Res. Natl. Inst. Stand. Technol. **114**, 341 (2009).

[64] R. M. Moon, T. Riste, and W. C. Koehler, Polarization analysis of thermal-neutron scattering, Phys. Rev. **181**, 920 (1969).

[65] A. Q. R. Baron, H. Franz, A. Meyer, R. Rüffer, A. I. Chumakov, E. Burkel, and W. Petry, Quasielastic scattering of synchrotron radiation by time domain interferometry, Phys. Rev. Lett. **79**, 2823 (1997).

[66] G. V. Smirnov, General properties of nuclear resonant scattering, Hyperfine Interact. **123/124**, 31 (1999).

[67] R. Waugh and E. A. Evans, Thermoelasticity of red blood cell membrane, Biophys. J. **26**, 115 (1979).

[68] R. H. Hochmuth, K. L. Buxbaum, and E. A. Evans, Temperature dependence of the viscoelastic recovery of red cell membrane, Biophys. J. **29**, 177 (1980).

[69] D. S. Heron, M. Shinitzky, M. Hershkowitz, and D. Samuel, Lipid fluidity markedly modulates the binding of serotonin to mouse brain membranes, Proc. Natl. Acad. Sci. USA **77**, 7463 (1980).

[70] C. A. Stanich, A. R. Honerkamp-Smith, G. G. Putzel, C. S. Warth, A. K. Lamprecht, P. Mandal, E. Mann, T. A. D. Hua, and S. L. Keller, Coarsening dynamics of domains in lipid membranes, Biophys. J. **105**, 444 (2013).